

# A New Position Reconstruction Method for Position Sensitive Photomultipliers

Maria Mikeli, Athanasia Polychronopoulou, Alexander Gektin, Nikos Giokaris, Andreas Karabarounis, Dimitris Maintas, Costas N. Papanicolas, Vyacheslav Pedash, Dimitris Thanasis and Efstathios Stiliaris

**Abstract**—A new position reconstruction method for position sensitive photomultiplier tubes is proposed in this work. The algorithm is based on a mathematical model operating on the charge signals recorded from the anode wires of a multi-wired anode system. This method overcomes the usual irregularities produced by the center of gravity algorithm near the edges of the field of view, especially when a homogeneous scintillation crystal is used. According to this method, the amount of the detected charge on a multi-wired anode system is calculated from the light distribution on the photo-cathode assuming a superimpose of analytically defined Gauss curves and a constant amplification of the photomultiplier tube. The parameters of this expression are experimentally defined on an event-by-event analysis by performing all required transformations. Data are obtained from a small field, high resolution  $\gamma$ -Camera system with a 16X+16Y multi-wired crossed anode using the Position Sensitive Photomultiplier Tube (PSPMT R2486, HAMAMATSU). The optical photon distribution for each type of the scintillation crystal used in the experiment is calculated with the photon transport system DETECT2000. Systematic measurements for a group of inorganic scintillations crystals of CsI(Tl) with 2mm-4mm-8mm-12mm and 20mm in thickness, as well as of BGO with 2mm-3mm-5mm and 8mm in thickness, have been performed for different radiation sources ( $^{60}\text{Co}$ ,  $^{137}\text{Cs}$ ,  $^{99m}\text{Tc}$ ). The experimentally obtained parameters for the produced light distribution inside the various crystals are expressed and categorized according to the crystal geometrical characteristics. The developed method seems to drastically improve the resolution of the reconstructed planar information, even when homogeneous scintillation crystals are used.

## I. INTRODUCTION

THE basic reactions which occur when radiation encounters matter and the effects produced by these processes

This work is partially supported by the General Secretariat for Research and Technology Hellas through the Greek-Ukraine bilateral program. It is also partially supported by the 03EΔ287 research project, implemented within the framework of the "Reinforcement Programme of Human Research Manpower" (PENED) and co-financed by National and Community Funds (25% from the Greek Ministry of Development-General Secretariat of Research and Technology and 75% from E.U.-European Social Fund). The financial support by the program KAPODISTRIAS (Special Account for Research Grants) of the National and Kapodistrian University of Athens is gratefully acknowledged.

M. Mikeli, A. Polychronopoulou, N. Giokaris, A. Karabarounis, C.N. Papanicolas, D. Thanasis and E. Stiliaris are with the National and Kapodistrian University of Athens, Department of Physics, 15771 Athens, Greece.

N. Giokaris, A. Karabarounis, C.N. Papanicolas and E. Stiliaris are additionally with the Institute of Accelerating Systems & Applications (IASA), Athens, Greece.

D. Maintas is with the Institute of Isotopic Studies, Athens, Greece.

A. Gektin and V. Pedash are with the Institute for Scintillation Materials, Kharkov, Ukraine

Corresponding author: E. Stiliaris (e-mail: stiliaris@phys.uoa.gr)

are well known. However, in Single Photon Emission Computed Tomography (SPECT) and generally in  $\gamma$ -ray imaging, it is important to determine the exact position in space of the photo-conversion. Compared to the plane, defined by the two transversal coordinates parallel to the photo-detectors entrance window, the coordinate normal to it, called the Depth Of Interaction (DOI), remains unspecified [1], [2]. This leads in a parallax error and as a result to a non-uniform and non-isotropic spatial resolution. For existing  $\gamma$ -ray imaging systems, the image quality can be improved potentially if a sufficiently good estimate of DOI is provided by the detector. Many techniques have been proposed for studying such a detector; their common philosophy is based on the determination of the light distribution on the entrance window of the photodetector as stated for example in [3] and [4].

Apart from the DOI problem, another factor which affects the quality of the spatial resolution in most of the  $\gamma$ -imaging systems arises from the usage of traditional reconstruction algorithms, lacking the necessary ability to correctly handle the detected information especially near the limits of the field of view.

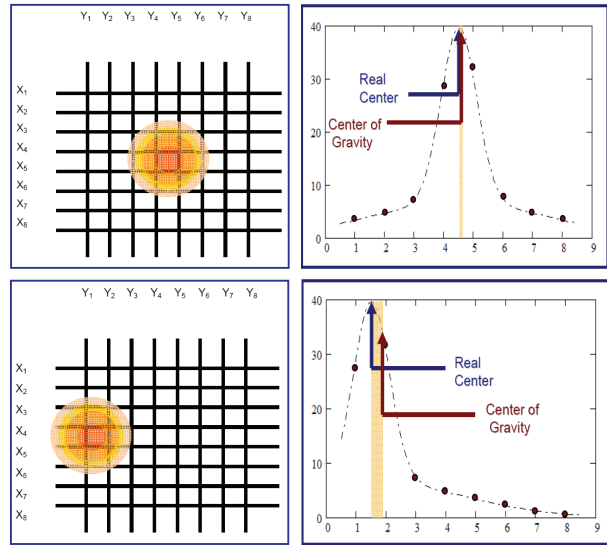


Fig. 1. The distribution of the electron cloud for a central and a non-central event. Due to the unbalanced charge for a non-central event, the traditional charge center of gravity algorithm reconstructs incorrectly the position.

The traditional charge center of gravity algorithm (Anger algorithm) operates successfully in the case of a centrally detected  $\gamma$ -ray, but not satisfactorily in the case of an electron cloud positioned near the edge of the anode, as shown in Fig. 1, where the unbalanced amount of the charge produces systematical shifts towards the center of the image and reduces the effective field of view. As a consequence, on the boundary region a barreloid deformation occurs [5] and the traditional charge center of gravity equations for position reconstruction

$$X_{pos} = \frac{\sum_{i=1}^N i Qx_i}{\sum_{i=1}^N Qx_i} \quad \text{and} \quad Y_{pos} = \frac{\sum_{i=1}^N i Qy_i}{\sum_{i=1}^N Qy_i}$$

result to a non-uniform and non-isotropic spatial resolution. The planar image can potentially be improved by using a position reconstruction algorithm suitable for the whole field of view of the camera.

The main purpose of this study is firstly the inquiry of the correlation of the DOI and the light distribution in both continuous and pixelated scintillation crystals and secondly, a simple modeling of the charge distribution detected by a Position Sensitive Photomultiplier Tube (PSPMT) for a given scintillation light distribution. Based on these results a new position reconstruction algorithm for a uniform and isotropic spatial resolution will be introduced.

## II. OPTICAL SIMULATIONS

Monte Carlo simulations for determining the optical photon distribution for continuous and pixelated scintillation crystals were performed using the photon transport program DETECT2000 [6].

DETECT2000 models the behavior of optical systems and particularly scintillation detectors. It generates individual scintillation photons in specified portions of the scintillator. Afterwards, it follows each photon in its passage through the various components and interactions with surfaces and records the fate (absorption, escape or detection) of each, along with its decay and delay times, total elapsed time to detection, number of reflecting surfaces encountered, last coordinates and whether or not the photon was wavelength shifted. The program uses initial definition statements to specify the optical properties of all materials and surface finishes used in the simulation. Components are then built out of these materials and surface finishes. The optical behaviour of each surface is chosen by selecting one of a set of predefined surface finishes. Surfaces in optical contact are taking into account Snell's law

$$\frac{\sin(\theta_i)}{\sin(\theta_t)} = \frac{n_2}{n_1}$$

and the optical properties of the various surfaces such as the index of refraction and the reflection coefficient.

In this work, a CsI(Tl) continuous crystal, 4 mm thick and of 25 mm radius was initially simulated, together with a 3 mm of pyrex glass placed before the detective surface and representing the entrance window of the Position Sensitive Photomultiplier Tube (Fig. 2a).

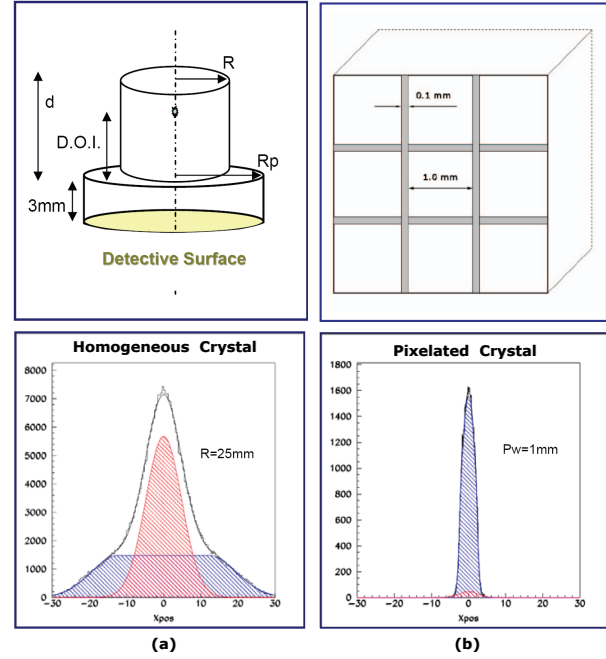


Fig. 2. Optical simulation of continuous and pixelated scintillator prototypes with the program DETECT 2000. (a) Geometry of the simulated homogeneous crystal with the entrance window of the photomultiplier and the produced photon distribution along the x-axis. (b) Part of a pixelated scintillator crystal (3x3 pixels) and the x-axis projection of the detected photons. The spread of the light in the homogeneous crystal is clearly shown.

The optical photons were generated isotropically by a point source located on the crystal axis at a small distance from the PSPMT entrance window [7]. A typical x-position distribution of the collected light is shown in Fig. 2a, where the narrow Gaussian curve may be thought as the curve that represents the photons that have not been reflected and the wide one, constituted of a constant part (plateau) and two Gaussian edges, represents the reflected photons.

Secondly, a pixelated CsI(Tl) crystal as the one shown in Fig. 2b was simulated, where the width of the squared pixels was 1 mm and the epoxy placed between them was 0.1 mm thick. The optical photons were generated inside the central pixel from a membrane like source with the transverse dimensions fitting the ones of the pixel. Again, a typical x-position distribution of the collected light is given in Fig. 2b; in contrast with the previous case, most of the generated photons are guided through the reflective sides of the scintillator pixel forming a narrow Gaussian shape on the detective surface.

Simulations of both continuous and pixelated crystals, show the dependence of the optical photon distribution on the Depth of Interaction, the pixel width and the photon source dimensions (Fig. 3). These results can be summarized as follows:

- In the case of homogeneous scintillation crystals, the width of the detected photon distribution (narrow Gauss curve) shows an increasing trend with the Depth of Interaction (DOI), the last measured from the detective

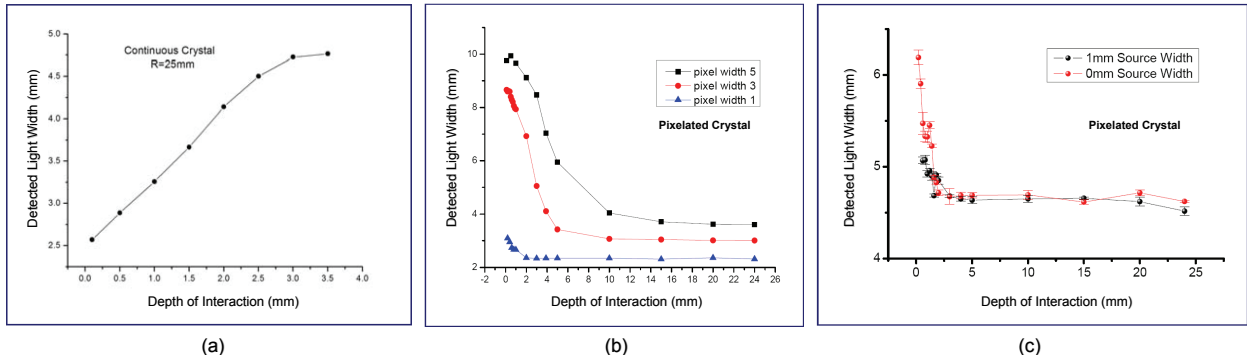


Fig. 3. Simulation results: (a) The dependence of the width of the light distribution on the Depth of Interaction for homogenous crystals. (b) The same for pixelated crystals and for various pixel sizes. (c) As previously, but for two different source dimensions.

surface of the photomultiplier. For a given value, which is mainly correlated with the radius of the cylindrically shaped crystal, a saturated behaviour is detected.

- In the pixelated crystals, the active size of each pixel determines asymptotically the width of the detected light on the photomultiplier surface. For small *aspect ratio* values (DOI relative to the pixel size), i.e. for  $\gamma$ -ray absorption near the detective surface, the distribution becomes large, due to escaped reflections off the pixel edges.
- The photon source dimension (generation volume) in the case of pixelated crystals does not show any influence on the measured light distribution, insofar the aspect ratio is kept at large values ( $> 1$ ).

### III. MODELING THE ELECTRON CLOUD

#### A. The Formalism

Taking into account the results of the simulation presented in the previous section, the light distribution on the detective surface of the photomultiplier entrance follows a functional approach of two canonical superimposed components. It is therefore legitimate to model the light density on the detective plane ( $x, y$ ) with a 2-dimensional function  $G(P_x, P_y, x, y)$  (Fig. 4, left) resulting from two Gaussian curves of different intensity and width:

$$G(P_x, P_y, x, y) = G_1(P_x, P_y, x, y) + G_2(P_x, P_y, x, y)$$

with

$$G_1(P_x, P_y, x, y) = A_1 \exp \left[ -\frac{(x - P_x)^2 + (y - P_y)^2}{2\sigma_1^2} \right]$$

$$G_2(P_x, P_y, x, y) = A_2 \exp \left[ -\frac{(x - P_x)^2 + (y - P_y)^2}{2\sigma_2^2} \right]$$

The parameters ( $A_1, \sigma_1, A_2, \sigma_2$ ) are characteristics of the light pulse produced by the scintillator in use and they must remain constant for every detected  $\gamma$ -ray independently of the falling position ( $P_x, P_y$ ) on the detector. In order to

calculate the charge accumulated by the multi-anode wires, assuming a constant photo-electron conversion and a constant amplification  $k$  inside the photomultiplier tube, the electron cloud has to be integrated according to the relations:

$$Q_{xi} = k \int_{y_1}^{y_2} G(P_x, P_y, x_i, y) dy \quad (x - \text{direction})$$

$$Q_{yi} = k \int_{x_1}^{x_2} G(P_x, P_y, x, y_i) dx \quad (y - \text{direction})$$

Determining experimentally the charge distribution allows the direct measurement of the intensity and width for the incident optical photons and consequently the verification of this assumption. From the charge collected by the individual wires ( $Q_{x1}, Q_{x2}, \dots, Q_{xN}$ ) and ( $Q_{y1}, Q_{y2}, \dots, Q_{yN}$ ) and by inverting the previous relations the parameter set ( $A_1, \sigma_1, A_2, \sigma_2$ ) can be experimentally defined.

An application example [7] of the introduced model is shown in the right part of Fig. 4. Comparison with experi-

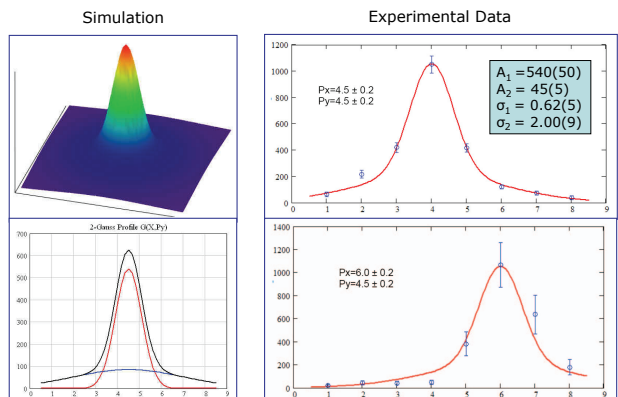


Fig. 4. Left: Optical photon distribution on the detective surface according to the introduced model and the resulting accumulated charge along the projection axis. Right: Model description of measured charges for any incident position on the detector surface by fitting once the free parameters of the model. Shown is a central and a non-central measured event; both are described with the same set of parameters.

mental results fixes the free parameter set for central position events located at ( $P_x=4.5$ ,  $P_y = 4.5$ ). Keeping this parameter set unchanged the charge distribution can be adequately reproduced for any other incident position as shown for example in the lower diagram for the case ( $P_x=6.0$ ,  $P_y = 4.5$ ). This methodology incorporates of course the DOI problem of the crystal as discussed in the introduction. In order to study the validity of the introduced formalism by eliminating any influence of DOI uncertainties a control procedure as described in the next section has been performed.

### B. Experimental Control

The validation of the introduced formalism has been checked with an experimental setup, where control light pulses are produced by a green LED. A grid with equidistant holes is used in front of the PSPMT to guide a small fiber glass carrying the control light pulses as shown in Fig. 5. The advantage of this method is two-fold: Firstly, the characteristics of the light distribution are constant for all events and secondly, the position of the guided light pulses is *a-priori* well known with high accuracy.

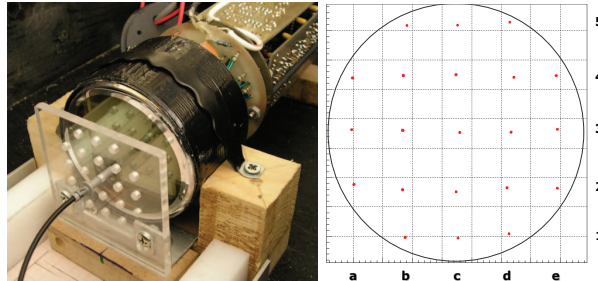


Fig. 5. Experimental control with light pulses: A grid with equidistant holes is used in front of the PSPMT to guide control light pulses produced by a green LED. The reconstructed 21 positions indicated by the columns  $\{a,b,c,d,e\}$  and the rows  $\{1,2,3,4,5\}$  are shown in the right figure.

The grid comprises a total of 21 positions from a square  $5 \times 5$  matrix, placed 10 mm apart each other simply indicated by the columns  $\{a,b,c,d,e\}$  and the rows  $\{1,2,3,4,5\}$ . Due to the cylindrical shape of the photomultiplier window the four edges (a1,a5,e1,e5) of the square matrix are not used. A reconstructed planar image of the detected light pulses for all valid grid positions is shown in the right part of Fig. 5.

Using the R2486 model of the HAMAMATSU PSPMT with the  $16X+16Y$  wired anode, where for simplicity reasons every two wires are connected together, the  $Q_{xi}$  and  $Q_{yi}$  ( $i=1\dots 8$ ) charge distribution have been measured for each of the grid positions. Based on the introduced model and with an inverse procedure, the light emission parameters ( $A_1, \sigma_1, A_2, \sigma_2$ ) are best estimated from all data points. With a fixed set of values the charge distribution is calculated and directly compared to the measured values. As shown in Fig. 6, a reasonable agreement for the whole effective area of the Position Sensitive Photomultiplier Tube and for both directions is achieved.

### IV. POSITION RECONSTRUCTION ALGORITHM

To overcome the difficulties in the position reconstruction discussed in the introduction, two different solution schemes are proposed. According to the presented electron cloud model, the fitted parameter set can be extended to include additionally the center coordinates ( $P_x, P_y$ ) of the optical photon distribution. Thus, for each detected event consisting of totally 16 measured values (8X+8Y charges), the six parameter set ( $P_x, P_y, A_1, \sigma_1, A_2, \sigma_2$ ) is easily fixed. Consequently the ( $P_x, P_y$ ) can be further used as the reconstructed position. This scheme requires obviously the arithmetic inversion of the presented formalism and consumes much of the computational time; therefore only an offline algorithmic implementation is possible. A much simpler scheme for reconstruction purposes can be applied following the example of the charge distribution shown in Fig. 1: A function formed by the overlap of two Gaussian curves, similar to the previously introduced but one-dimensional  $G(P_x, P_y, x, y)$  function, can define the center ( $P_{x0}, P_{y0}$ ) of the distribution and yields to more accurate results than that of the traditional reconstruction algorithm ( $X_{pos}, Y_{pos}$ ). The first, exact method is referred in the following as the *Inverse Model Fit*, while the second, simpler one as the *Gauss Fit*.

#### A. Measured Light Distribution in Scintillation Crystals

Various inorganic homogeneous crystals CsI(Tl) and BGO, as well as a CsI(Tl) pixelated one, have been irradiated with  $\gamma$ -sources. Based on the previously described procedure the generated light distribution inside the scintillators has been investigated from the measured charge distribution on the multi-wired PSPMT anode. One gauss distribution is sufficient to describe the light in all homogeneous crystals; due to the strong reflective effects the pixelated crystal demands the full set of the two-gaussian distribution. The best fitted set of the  $(A, \sigma)$  parameters is defined for each combination of scintillator and the  $\gamma$ -source. As expected, there is a strong correlation between the experimentally defined  $\sigma$  value of the light distribution inside the scintillator and its thickness. A typical result is shown in Fig. 7 for the measured set of the homogeneous CsI(Tl) crystals and for three different  $\gamma$ -radiation sources.

Light distribution parameters have been defined for both sets of the CsI(Tl)  $\{2mm-4mm-8mm-12mm-20mm\}$  and the BGO  $\{2mm-3mm-5mm-8mm\}$  homogeneous crystals, as well as for the CsI(Tl) 4mm pixelated one. The three  $\gamma$ -radiation sources used in this experiment were  $^{60}Co$ ,  $^{137}Cs$  and  $^{99m}Tc$ . For comparison, the parameter set for the pixelated CsI(Tl) crystal and the  $^{60}Co$ -source is found  $A_1/A_2 = 8.0 \pm 2.4$ ,  $\sigma_1 = 0.59 \pm 0.14$  and  $\sigma_2 = 2.7 \pm 0.6$ .

#### B. Reconstruction Results with Homogeneous Crystals

In order to verify the new algorithms' success, a number of experiments were performed. Data were obtained from a small field, high resolution  $\gamma$ -Camera system with a multi-wired crossed anode using the R2486 (HAMAMATSU) PSPMT. Fig. 8 presents a typical result of a raw planar image for three

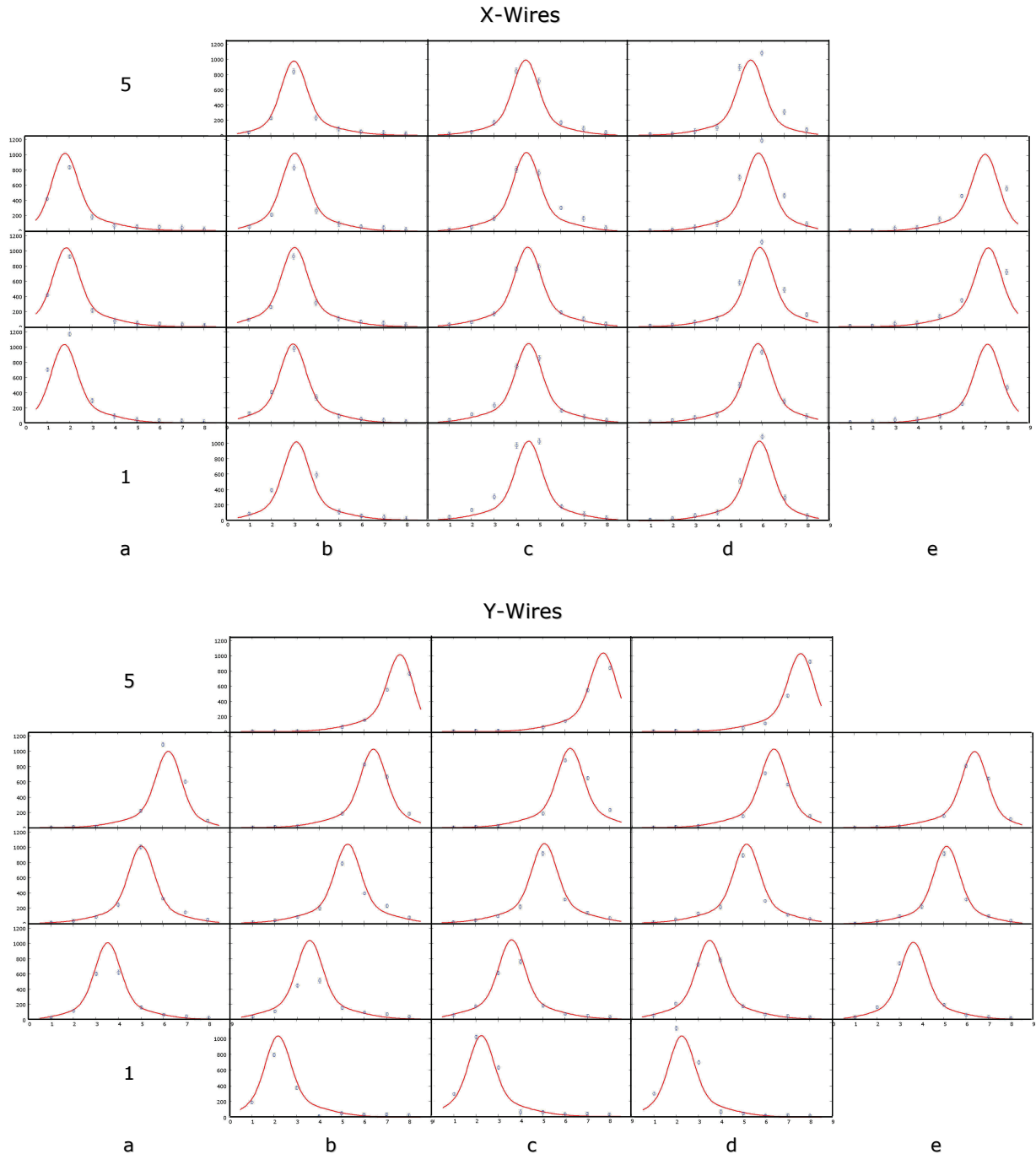


Fig. 6. Experimental control with light pulses: The charge distribution is measured for all the grid positions and with an inverse procedure based on the introduced model the light emission parameters are best estimated. With a fixed set of the  $(A_1, \sigma_1, A_2, \sigma_2)$  values the charge distribution is calculated (red lines) and directly compared to the measured values (blue points). A reasonable agreement for the whole effective area of the Position Sensitive Photomultiplier Tube is achieved.

capillaries filled with  $^{99m}Tc$  solution and placed parallel in front of the lead collimator at distances  $d_1 = 6.0\text{ mm}$  and  $d_2 = 7.2\text{ mm}$  to each other. In the depicted example the 2 mm CsI(Tl) homogeneous crystal is used.

This planar image is reconstructed in three different ways: With the traditional (Anger), the 1-Gauss Fit and the here introduced Inverse Model Fit reconstruction. This example reveals the advantages of the new reconstruction algorithms.

## V. CONCLUDING REMARKS

The study of the light distribution from a scintillation crystal and its characterization indicates that it is strongly correlated to both the Depth of Interaction (DOI) and the geometrical properties of the system. The results of this study have shown that the DOI affects the width of the distribution while the crystal's shape seems to affect both the shape and the width. The experimentally collected charge, which depends on the electrons' cloud position, is the basis for a new position reconstruction algorithm that results in a more accurate and uniform spatial resolution. The new model applied in both homogeneous and pixelated crystals, resulted in a uniform spatial resolution overcoming the traditional charge center of gravity algorithmic disadvantages.

## VI. ACKNOWLEDGMENT

We would like to thank Y. Grammenos (IASA) for his technical help during the mechanical setup of the experimental work and J. Laspas (Institute of Isotopic Studies) for providing the  $^{99m}\text{Tc}$  water solutions used in the experiments.

## REFERENCES

- [1] Ch.W. Lerche *et al.*, "Depth of  $\gamma$ -Ray Interaction Within Continuous Crystals from the Width of its Scintillation Light-Distribution", *IEEE Transactions on Nuclear Science*, Vol. 52, pp. 560–572, 2005.
- [2] Ch.W. Lerche *et al.*, "Depth of interaction detection with enhanced position-sensitive proportional resistor network", *Nucl. Instrum. & Methods A*, Vol. 537, pp. 326–330, 2005.
- [3] A.P. Dhanasopon *et al.*, "Scintillation Crystal Design Features for a Miniature Gamma Ray Camera", *IEEE Transactions on Nuclear Science*, Vol. 52, pp. 1439–1446, 2005.
- [4] L. Perera, M. Lerch, A. Rosenfeld, S.R. Meikle and J. Chan, "Spatial Resolution of a Small Cubic LYSO Scintillator Crystal Detector with Depth-of-Interaction Capabilities in a Small Animal PET Scanner", *IEEE Nuclear Science Symposium Conference Record*, pp. 3754–3759, 2007.
- [5] D. Thanasis *et al.*, "A Correction Method of the Spatial Distortion in Planar Images from  $\gamma$ -Camera Systems", Proceedings of the 4th International Conference on Imaging Technologies in Biomedical Sciences (ITBS-2007), Milos Island, 22–28 September 2007.
- [6] C. Moison, F. Cayouet and G. McDonald, "DETECT2000: A Program for Modeling Optical Properties of Scintillators", Version 5, September 1, 2000.
- [7] A. Polychronopoulou, "Study of Homogeneous and Pixelated Inorganic Scintillation Crystals for Tomographic Applications", MSc Thesis (in greek), Physics Department, National & Kapodistrian University of Athens, 2008.

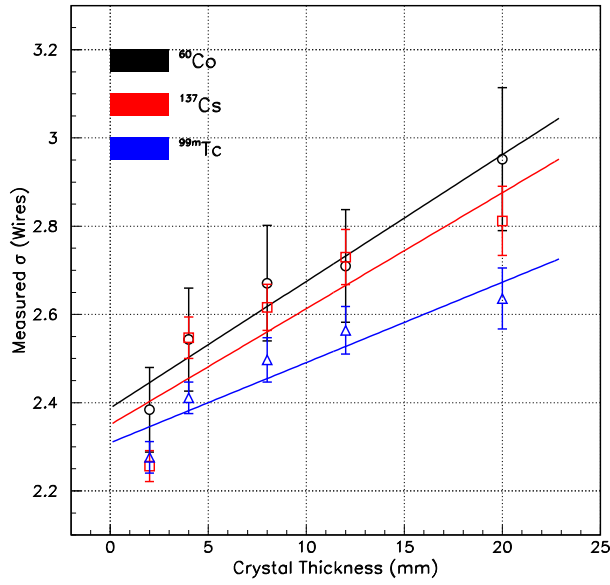


Fig. 7. Measured light distribution width ( $\sigma$ ) in various CsI(Tl) homogeneous crystals for three different  $\gamma$ -radiation sources. The unit in  $\sigma$  is defined in wire-distance (6mm).

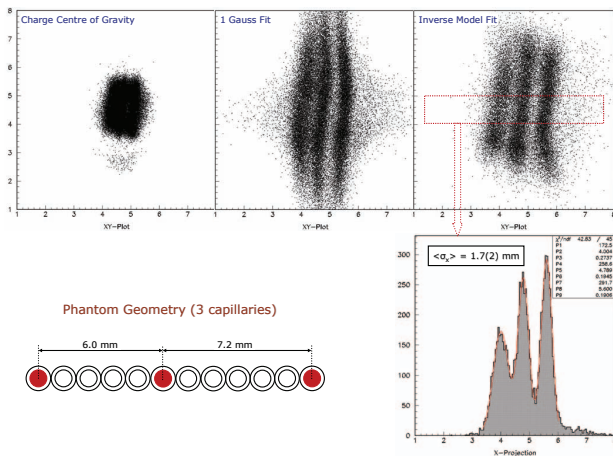


Fig. 8. Raw planar images from three parallel capillaries filled with  $^{99m}\text{Tc}$  solution using the 2 mm homogenous CsI(Tl) crystal. The phantom geometry is shown in bottom-left part of the picture. Three different algorithms are used to reconstruct the image: The traditional (Anger) center of gravity algorithm, the 1-Gauss Fit and the Inverse Model Fit introduced in this work. Only the two last algorithms can resolve the capillaries.

In contrast to the traditional methodology only the new algorithmic approach can resolve the capillaries. Based on the phantom distances between the three capillaries a first estimate for the spatial resolution along the x-direction gives the value  $\langle \sigma_x \rangle = 1.7 \pm 0.2 \text{ mm}$ . Similar results are also obtained and for the y-direction.